IEEE Access
Multidisciplinary | Rapid Review | Open Access Journal

Received 19 October 2024, accepted 10 November 2024, date of publication 13 November 2024,
date of current version 26 November 2024.

Digital Object Identifier 10.1109/ACCESS.2024.3497664

RESEARCH ARTICLE

Reconfigurable and Broadband Analog Computing With Terahertz Metasurface Based on Electrical Tuning of Vanadium-Dioxide Resonators

MOHAMMAD ALI SHAMELI[1,2], MIRKO MAGAROTTO[2], (Member, IEEE), ANTONIO-D CAPOBIANCO[2,3], (Member, IEEE), LUCA SCHENATO[2,3], (Member, IEEE), MARCO SANTAGIUSTINA[2,3], (Member, IEEE), MARIA ANTONIETTA VINCENTI[4], (Member, IEEE), AND DOMENICO DE CEGLIA[3,4,5], (Member, IEEE)

[1]Faculty of Electrical Engineering, K. N. Toosi University of Technology, Tehran 1541849611, Iran
[2]Department of Information Engineering, University of Padova, 35131 Padua, Italy
[3]National Inter-University Consortium for Telecommunications, CNIT, 43124 Parma, Italy
[4]Department of Information Engineering, University of Brescia, 25123 Brescia, Italy
[5]National Institute of Optics–National Research Council, 25123 Brescia, Italy

Corresponding author: Mohammad Ali Shameli (Mohammadali.shameli@unipd.it)

This work was supported in part by the Ministero dell'Istruzione e del Merito (MIUR) through the project Progetti di Rilevante Interesse Nazionale (PRIN) 2022 "PILLARS;" in part by the European Union under the Italian National Recovery and Resilience Plan (NRRP) Mission 4, Component 2, Investment 1.3, partnership on "Telecommunications of the Future" [program "RESearch and innovation on future Telecommunications systems and networks, to make Italy more smART (RESTART)"] under Grant CUP C93C22005250001 and Grant PE00000001; and in part by the Italian Ministry of University and Research (MUR) through eFficient pLasmA Intelligent Reflecting Surface (FLAIRS) under Grant PRIN 2022 PNRR P2022RFF9K.

ABSTRACT A architecture of reconfigurable analog computing devices is proposed for image processing and advanced wireless communication systems, such as those required for self-driving cars. This architecture is designed to work in the terahertz frequency range, and it is based on a metasurface made of VO_2 brick resonators as metaatoms. The system is capable of performing first-order and second-order derivative, or it may act as a mirror for impinging signals in a broad range of terahertz frequencies. The reconfigurability between these functions is achieved by tuning the temperature of the VO_2 resonators, which can be switched between the metallic and the insulator state with an electric current passed through a back metal layer. Following this approach, we present two dynamically controlled metasurfaces, one designed in k-space and the other in real-space.

INDEX TERMS Analog computing, reconfigurable devices, vanadium dioxide, first and second-order derivative, nonlocal metasurface, wide bandwidth.

I. INTRODUCTION

The pace of creating, processing, and storing data has remarkably increased worldwide in the past few years. Also, fifth-generation (5G) and sixth-generation (6G) wireless communication systems and the advent of new technologies such as autonomous driving and the rapid development of technologies related to artificial intelligence, demand large data file processing [1], [2]. In the past few decades, digital processing has been widely used for these computational tasks due to its reliability and high-speed operation. However, low performance at high frequency, high power consumption, and the difficulties in analog to digital conversion and vice versa pose important challenges that lead researchers to leverage analog computing as an alternative to perform common computational tasks such as differentiation, integration,

The associate editor coordinating the review of this manuscript and approving it for publication was Wanchen Yang.

solution of differential equations, as well as fundamental image processing operations such as edge detection [3], [4]. Also, in optical frequency, analog computing has an application in image processing, such as edge detection for microscopy imaging, quantum imaging, and holographic imaging [5]. Using optical analog communications instead of digital ones can reduce energy consumption and increase communication speed between two points without needing analog-to-digital and vice versa conversion [6]. Also, optical analog computing has been used in artificial intelligence models, such as feedforward neural networks, reservoir computing, and spiking neural networks, due to low energy consumption, broad bandwidth, and low latency [7].

Metasurfaces, owing to their ability of wave-front control and reliable fabrication processes [8], [9], [10], [11], are the best choice to realize such a significant task [1], [3], [4], [12], [13], [14], [15], [16], [17]. These structures have many applications in different frequency bands [18], [19], [20]. A metasurface with a U-shaped split-ring resonator and a fork-shaped resonator has been used for Multi-band electromagnetically induced transparency (EIT) in the terahertz regime [18]. Another metasurface is used in the microwave frequency to apply power reception [19]. Metasurface and metamaterial structures can be applied for absorber applications, especially in optical wavelengths [20]. For instance, an intelligent, lightweight, and compact edge-enhanced depth perception system is realized with binocular meta-lens for spatial computing at the wavelength of 532 nm [21]. Also, other work proposed a dielectric metasurface composed of quasi-continuous nanostrips that could overcome the limitations of broadband and highly efficient structures simultaneously in comparison with traditional metasurfaces with discrete resonators [22]. In refs. [3], [12], and [13] a first-order differentiator metasurface was designed using dielectric and metallic brick resonators. The second-order differentiator with a high numerical aperture, which is appropriate for edge detection, has been realized using a metasurface with a honeycomb structure without dependency on polarization [1]. Cordaro et al. [14] proposed a second-order differentiator on the input image for edge detection applications with a silicon metasurface. Kwon et al. [15] presented a nonlocal metasurface with a split ring resonator for first- and second-order differentiation and integration. A metasurface as a silicon-on-insulator platform, capable of integration in the spatial domain, was designed and fabricated [4]. Estakhri and his collaborators introduced a metamaterial platform to provide a fast and chip-scale design capable of solving integral equations [16]. Despite all these efforts, the absence of reconfigurability, which is essential for high data rates in intelligent wireless communication systems, is a significant disadvantage.

Although increasing demand for reconfigurable devices in analog computing, researchers have made a few proposals in recent years. Momeni et al. suggested a promising path toward spatiotemporal computing using graphene metasurfaces in both space and time domains that can tune performance by applying an external voltage to monolayer graphene [17]. Another work demonstrated a reconfigurable metasurface that can mechanically tune between low-pass filter, high-pass filter, and second-order differentiator [23]. A photonic signal processor with the ability of signal processing functions, including differentiation, integration, and Hilbert transformation, has been achieved by controlling the injection current to the active component of the structure [24]. Babashah et al. proposed a reconfigurable photonic integrated signal processing system that can control different performances, including Fourier transform, first-order derivative, integration, and convolution using the desired arbitrary transfer function through a cascaded Mach-Zehnder modulator and a phase modulator [25]. Using memristive devices, Yunning designed and fabricated Field-programmable analog arrays for analog computing at the kilohertz frequencies [26]. An additional contribution at optical telecommunication wavelengths (1550 nm) involves the implementation of reconfigurable photonic integrated computing [27]. This system, structured on a quadrilateral topology network, can execute temporal differentiation, integration, and Hilbert transformation within a substantial bandwidth of 40 GHz. Despite these efforts, drawbacks such as complexity and feasibility [17], [27], large volume occupation [24], [25], and mechanical reconfigurability rather than an electrical one [23] are serious obstacles toward the realization of reliable tunable analog computing.

To address these issues, we propose and numerically test a new strategy to achieve reconfigurable analog computing devices by using a VO_2 metasurface at terahertz (THz) frequencies. The tunability of VO_2 at THz frequencies is very deep. Indeed, the conductivity switches from 2 S/m to 1×10^5 S/m [28] around the temperature of 68°C, however, in the heating process insulator to metal transition occurs at one or two degrees higher, and in the cooling process, the transition from metal to insulator is one or two degrees lower [29]. Above the critical temperature of approximately 68 °C, not only the electrical but also the optical properties undergo a significant change. In the lower temperatures, VO_2 is like an insulator without any loss, while increasing temperature to more than 68°C increases the imaginary part of the permittivity, as described by the Drude model [30], [31], [32]. Therefore, this frequency range is particularly appealing for devices with reconfigurable functionalities based on the phase transition in VO_2. In addition, there is a growing demand for tunable and reconfigurable devices for high-capacity wireless communications in the THz range for a wide variety of applications, including front- and backhauling of base stations, wireless local and personal area networks, near-field communications, wireless connections in data centers, and device-to-device communications [33]. In this work, we propose two designs to show the full potential of VO_2-based reconfigurable metasurfaces in the THz regime. In the first design, a metasurface with VO_2 brick

resonators, working in k-space, provides a first-order differentiator transform function in reflection when VO_2 is in the metallic state. Switching the VO_2 from the metallic state to the insulator state by reducing the temperature leads to changing the performance of the metasurface to self-reflection at the normal angle, like a mirror. In the second design, when the metasurface works in direct space, it can change between two states: second-order differentiator in the high-temperature state and mirror in the low-temperature state of the VO_2 brick resonators. Compared with previous works on reconfigurable analog computing, this structure is easy to fabricate, has an operational speed on the order of nanoseconds [34], and has an ultra-compact architecture in the THz regime.

The organization of this paper will start with the theory of analog computing and design a reconfigurable analog computing metasurface in k-space. Then it will be investigated using a full-wave simulation with the finite element (FEM) method in COMSOL Multiphysics. In the third section, we developed a compact analog computing device based on a reconfigurable nonlocal metasurface to investigate such structure in real space. These analog computing devices have applications in image processing, smart wireless systems, and self-driving cars. One of the challenges of this structure is increasing or decreasing the temperature of VO_2 resonators using the electric current passing through the back metal. Thus, the influence of changing temperature on other devices should be investigated when integrated into large communication or imaging systems.

II. ANALOG COMPUTING WITH VO_2 METASURFACE IN K-SPACE

In this section, we design mathematical operations in the Fourier space based on the building blocks represented in Fig. 1. Based on this figure, $f(x)$ and $g(x)$ are the arbitrary input and corresponding output of the system. The input signal passes through the lens as a spatial Fourier transform block and reaches the metasurface located in the Fourier plane of the lens. Then, it is convolved with the impulse response of the metasurface, and the filtered signal passes through the lens and is converted back to the real space. The lens used in the setup of Fig. 1 should be able to focus Terahertz beams. Commercial lenses for Terahertz radiation have dimensions ranging from 30 to 100 mm and focal lengths from 15 to 300 mm [35]. In the alternative, a metalens may be employed, with meta-atoms engineered to produce a converging lens effect with an effective focal length of a few centimeters [36]. In our analysis, we assume only one spatial dimension (x) and one-dimensional frequency space (k_x). In other words, $g(x)$, i.e., the output of the system, can be obtained as follows:

$$g(x) = h(x) * f(x) = \int h(x - x')f(x')\mathrm{d}x' \tag{1}$$

and the spatial Fourier transform of equation (1) is:

$$G(k_x) = H(k_x)F(k_x) \tag{2}$$

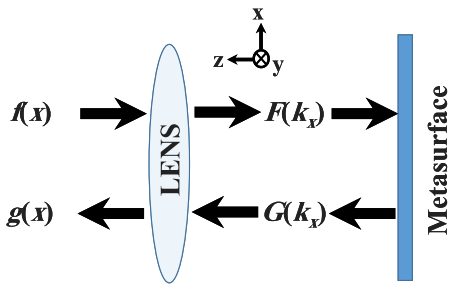

FIGURE 1. Sketch of the mathematical operation in Fourier space with a lens as a Fourier transform (FT) and a reflective reconfigurable metasurface.

where $G(k_x)$, $H(k_x)$, and $F(k_x)$ are the Fourier transforms of the $g(x)$, $h(x)$, and $f(x)$ respectively and k_x is the spatial frequency.

The proposed reconfigurable analog computing metasurface designed in Fourier space is shown in Fig. 2. The incident wave is $F(k_x)$, the Fourier transform of the $f(x)$, as an input of the system, and the reflection of the electric field is $G(k_x)$. Also, $H(k_x)$ is the transfer function associated with the target mathematical operation related to the k_x-dependent reflection coefficient of the reflective metasurface. To realize the target mathematical operation, the unit cells of the structure will be engineered based on the desired reflection associated with the proposed mathematical operation. Then, the reflection of the metasurface, located in the Fourier plane, passes through the lens and converts back to real space after two Fourier transforms. The domain of the reflected signal will be inverted due to the properties of the repeated Fourier transform ($FT\{FT[f_x(x)]\} \propto f_x(-\mathrm{x})$).

To realize the transform function, the engineered resonators should be distributed periodically on the supercell of

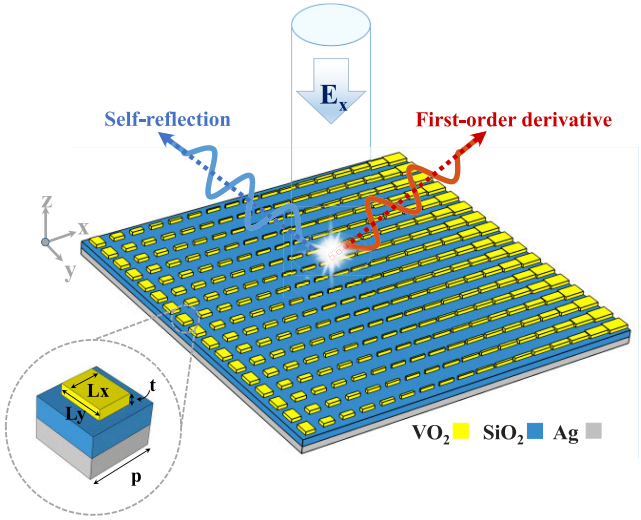

FIGURE 2. Perspective view of reconfigurable analog computing metasurface and its unit cell with VO_2 brick resonator, SiO_2 layer, and back metal made of Ag.

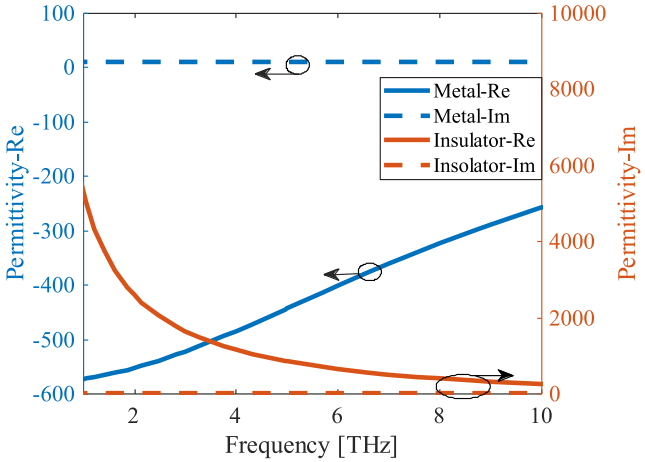

FIGURE 3. Real and imaginary part of the VO_2 permittivity between frequency of 1 THz and 10 THz in both metallic and insulator states.

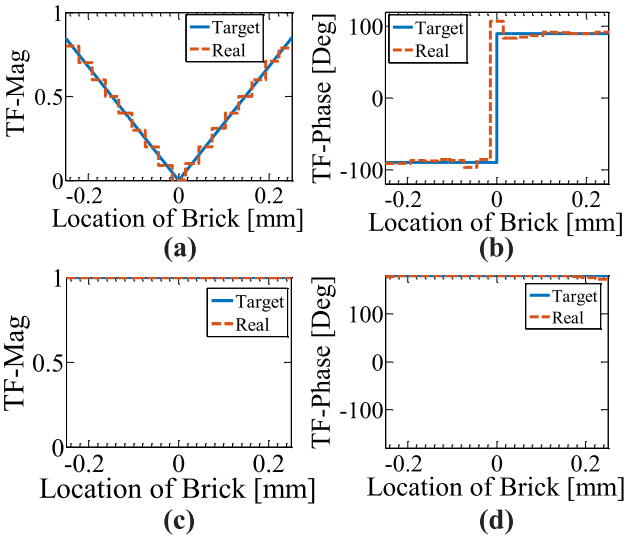

FIGURE 4. Target and actual electric field reflection profile of the reconfigurable metasurface at (a,b) high-temperature (first-order derivative) and (c,d) low-temperature (mirror).

the metasurface to create the desired amplitude and phase of the reflection. We consider plane wave excitation with x-polarization impinging normally on the metasurface at a frequency of 3.75 THz. The THz regime was chosen due to the good plasmonic properties of the VO_2 in the metallic state. The full-wave simulations are performed with the Finite Element Method (FEM) using the COMSOL software. The metaatom of the metasurface has a brick resonator made of VO_2 with lateral dimensions a, along the x-axis, b, along the y-axis and height $t = 300$ nm. The brick resonator is separated from the Ag substrate (with a height of $t_m = 10\ \mu$m) by an insulator layer of SiO_2 with permittivity of 2.1 (with a height $h = 10\ \mu$m), and the periodicity of the unit cell is $p = 30\ \mu$m. For VO_2, we consider a constant relative permittivity equal to 9 in the insulator state (below T_C). For the metallic state at high temperature, we use the frequency-dependent Drude model, $\varepsilon = \varepsilon_\infty - \omega_p^2/(\omega^2 - j\omega\gamma)$, with $\varepsilon_\infty = 12$, plasma frequency $\omega_p = 1.4 \times 10^{15}$ rad/s, and collision frequency $\gamma = 5.75 \times 10^{13}$ 1/s [30], [37], [38]. For Ag, the Drude model fitted to the experimental data reported in [39], is used. The parameters used in the Drude model are: $\varepsilon_\infty = 3.8$, the plasma frequency is $\omega_p = 3.8 \times 10^{16}$ rad/s, and the collision frequency is $\gamma = 2.7 \times 10^{13}$ 1/s. For the permittivity of silicon, data reported in [40] is used which considers both loss and frequency dispersion. To perform the target mathematical operation, the magnitude of the reflection should cover the range from 0 to 1, and the phase should be controlled between 0 degrees and 360 degrees. To achieve this goal, the lateral dimensions of the resonator are adjusted between 2 μm and 28 μm.

Here, we aim at the design of a tunable first-order differentiator. To design such a structure, we suppose two states of metallic and insulator at high temperature and low temperature of VO_2, respectively (see Fig. 3). Our goal is to design the first-order derivative at high-temperature thanks to the plasmonic effect of VO_2 at THz frequency through control of the amplitude and phase of reflection. According to the Fourier transform principle, the spatial derivative of $f(x)$ is related to its Fourier transform as follows:

$$FT\{\frac{d(f(x))}{dx}\} = (ik)F(k) \tag{3}$$

whose transformation should be provided by the reflective metasurface. As can be seen from Eq. (3), the spatial frequency (k) is unlimited; however, the length of the metasurface is limited, and the magnitude of the reflection coefficient must be below unity for energy conservation. To solve this problem, we assume that L is the finite extension of the metasurface in the x-axis direction (i.e., the dimension of the supercell), and we target the following normalized transfer function that realizes the first-order differentiator operation:

$$H(k) = (ik)/(L/2) \tag{4}$$

Using the data from the full-wave simulation at the high temperature of VO_2, the sizes of the brick resonators in the metallic state in the supercell (see Table 1) have been chosen to provide the target reflection profile of Eq. (4) via the plasmonic effect of VO_2 at THz frequencies. It is worth mentioning that the structure is not symmetric with respect to the plane $x = 0$, as required by the odd symmetry of the phase of the target transfer function. Fig. 4(a) and Fig. 4(b) show the target and actual reflection profiles (magnitude and phase) of the metasurface for the first-order derivative operation at high temperatures. The reflection profile of the actual structure, disregarding the discretization effect of the metasurface, perfectly overlaps the target one. As shown in Fig. 4(c) and Fig. 4(d), at low temperatures, when VO_2 is in the insulator state, no resonances are excited, and the interaction with the incident wave is quite weak. As a consequence, the metasurface works like a mirror and simply reflects the incident wave.

TABLE 1. The lateral dimensions of the VO_2 brick resonators that are distributed periodically in the supercell of the reconfigurable metasurface.

Res	*Lx* [μm]	*Ly* [μm]	Location [μm]
Res1	24	2	0
Res2	26	2.5	+30
Res3	26.5	3	+60
Res4	27	4	+90
Res5	27	5.5	+120
Res6	27.5	7	+150
Res7	28	9	+180
Res8	29	13	+210
Res9	29.5	18	+240
Res-2	21.5	2	-30
Res-3	20.5	2	-60
Res-4	19.7	3	-90
Res-5	19	4	-120
Res-6	18.2	5	-150
Res-7	17.3	7	-180
Res-8	16	10	-210
Res-9	14	18	-240

To investigate the performance of this reconfigurable device, the metasurface with periodic boundary conditions has been simulated in COMSOL Multiphysics®6.1 with the FEM method. In this simulation, as an illustrative example, the excitation is x-polarized, and it has the following: $E_x = (x/1e-4) \times exp(-(x/1e-4)^2)$ (see Fig. 5(a)) at a carrier frequency of 3.75 THz. We performed this simulation at a high and low temperature when VO_2 is in the metallic state and the insulator state, respectively. As shown in Fig. 5, the output of the system at the high temperature is the first-order derivative of the incident wave; as expected, in the low-temperature regime, the metasurface works like a mirror and reflects the incident wave towards the air side. The operational speed of this analog computing device is dependent on switching mechanisms for the VO_2 resonator. the first mechanism is ultrafast (100 femtoseconds), which is photo-induced, and that is only possible using high-intensity and short pulses as stimuli [41], and the second process which is used in our work is a slower one (nanosecond), purely thermal, that can be induced with electrical current, or heat [34].

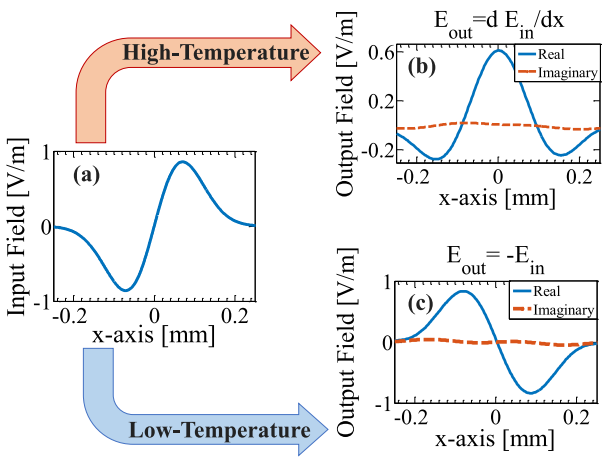

FIGURE 5. (a) The real part of the incident electric field (it has a zero imaginary part), (b) the output of the reconfigurable metasurface in high-temperature (first-order derivative), and (c) low-temperature.

III. ANALOG COMPUTING WITH VO_2 METASURFACE IN REAL-SPACE

In this section, we design a reconfigurable non-local metasurface [42], [43] that operates in direct space as a second-order differentiator at high temperatures and as a mirror at low temperatures. The non-local metasurface in the metallic state of VO_2 is designed in such a way that its output, i.e., the function of $g(x)$, is the convolution of the input, $f(x)$, and the second-order derivative of the impulse function (see Fig. 6(a)). In other words, the reflected field is the second-order derivative of the input field. In this configuration, we avoid using bulk lenses, and we work in real-space. Thus, the reconfigurable device is more compact than the previous one, which is designed to operate in the Fourier (or back focal) plane of a lens. The unit cell of the non-local metasurface is depicted in Fig. 6(b). Our goal is to tailor the reflection coefficient for impinging plane waves as a function of the angle of the incident to provide a transfer function of $G(k) \propto -k_x^2$ related to the second-order derivative. To provide such a transfer function, the lateral dimensions of the VO_2 brick resonators are determined based on parametric numerical simulations of COMSOL multiphysics®6.1 with the FEM method and setting periodic boundary conditions and plane wave as an excitation. Based on these investigations, the transfer function is shown in Fig. 6(a). The thickness of the resonator is $t = 50$ nm, and the lateral dimensions are set at $Lx = 26\ \mu$m and $Ly = 7\ \mu$m.

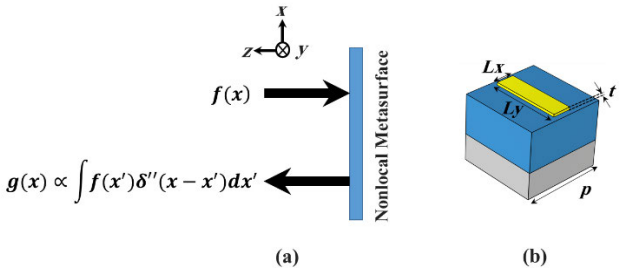

FIGURE 6. (a) Sketch mathematical operation in the real space with a non-local reflective reconfigurable metasurface. (b) Unit cell of reconfigurable non-local metasurface with VO_2 brick resonator, SiO_2 layer, and back metal made of Ag.

Figure 7(a) shows the transfer function of the second-order derivative at high temperatures. Also, at low temperatures (Fig. 7b), owing to the weak interaction of the incident wave with the VO_2 bricks in their insulator state, the transfer function is unity and only introduces a phase shift close to $-\pi$. To investigate the performance of this reconfigurable non-local metasurface, we use a numerical simulation with $E_x = exp(-(x/10^{-4})^2)$ at high and low temperatures when VO_2 is in the metallic and insulator states, respectively.

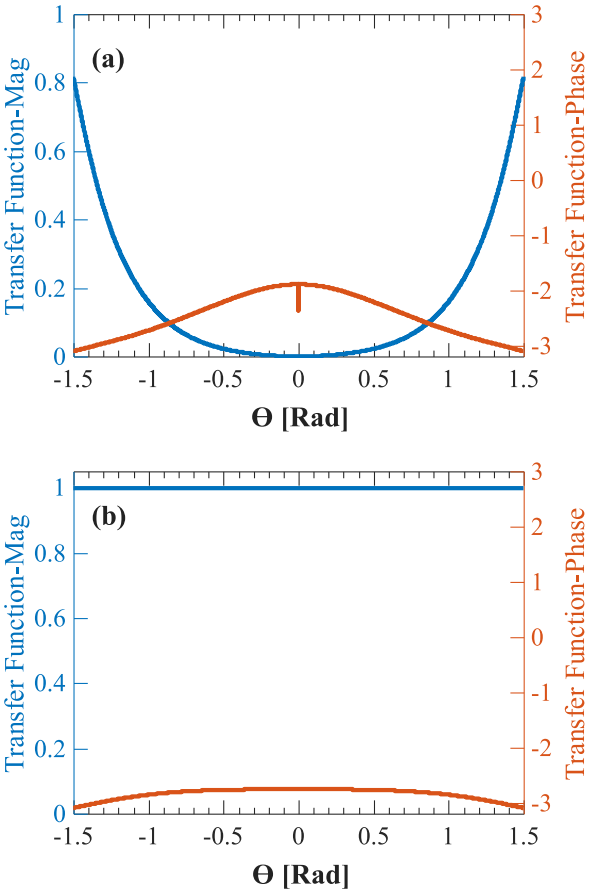

FIGURE 7. The transfer function of the reconfigurable non-local metasurface as a function of angle of incidence (θ) at (a) high temperature (second-order derivative) and (b) low temperature (mirror).

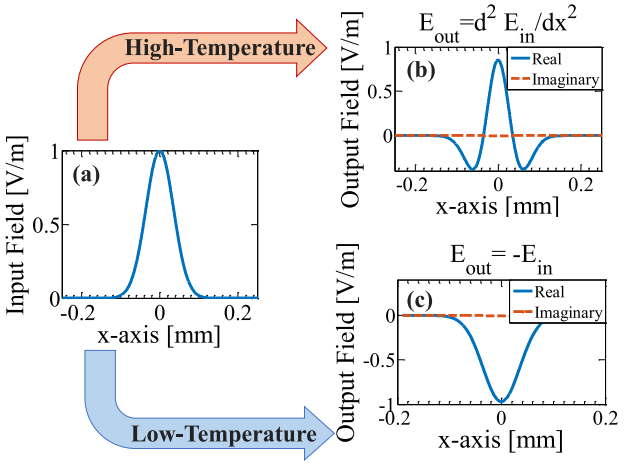

FIGURE 8. (a) The real part of the incident electric field (it has a zero imaginary part), (b) response of the reconfigurable non-local metasurface at high temperatures (second-order derivative), and (c) low temperatures.

TABLE 2. Comparing the properties of the proposed reconfigurable non-local metasurface with previous works.

Ref.	Structure	Functionality	Reconfigurable /Static	Bandwidth
[44]	Multi-layer Metasurface	Derivative	Static	-
[45]		Derivative	Static	5THz/200THz
[46]	Multi-layer Metasurface	Integrator	Static	-
[17]		Derivative	Reconfigurable	-
[27]	Photonic Circuit	Derivative/ Integrator	Reconfigurable	40GHz/193.5THz
This work	Metasurface	Derivative	Reconfigurable	2THz/3.5THz

As shown in Fig. 8, at high temperatures, the output of the system is a second-order derivative of the Gaussian beam; however, at low-temperature, the metasurface works like a mirror and reflects the incident wave to the air.

One of the significant advantages of this metasurface is that the transfer function remains almost unaltered in a large frequency range centered at around 3.5 THz, therefore providing a second-order derivative operation in a broadband frequency band of 2 THz (between 2.5 THz and 4.5 THz). As shown in Fig. 9(a), the magnitude of reflection becomes zero due to the dipole resonance in the operational frequencies, and the metasurface provides a second-order derivative transfer function of type $G(k) \propto -k_x^2$ in a broad range of frequencies. Also, based on Fig. 9(b), in each frequency at the bandwidth of the metasurface, the reflection phase is almost unchanged. To investigate the behavior of zero reflection at the proposed bandwidth, the normalized electric field is depicted at 3 THz, 3.4 THz, and 3.75 THz in Fig 9(c), showing the dipole resonance of the nano-brick. Based on the proposed calculations, this reconfigurable device not only has a wide relative bandwidth of approximately 2 THz with an average numerical aperture of 0.99 across this band. A large numerical aperture and a broadband operation are critical parameters in analog computing devices that perform operations such as differentiation and edge detection. Beyond being reconfigurable in the THz regime, the structure proposed here has a fractional bandwidth close to 50% and an average NA of approximately 0.99. The numerical aperture is defined as the angular spectrum range in which the response of the structure allows analog computing functionality. Namely, the second-derivative operator, which is $-k^2$ in the spectrum domain, is kept unaltered from approximately -90 to 90 degrees. Hence, the numerical aperture (NA $= \sin \alpha$, with α acceptance angular range), is equal to approximately 1.

Table 2 compares the properties of the reconfigurable non-local metasurface for analog computing applications with other similar works in terms of reconfigurability, functionality, and bandwidth. Based on this study, our analog computing device has the largest bandwidth compared to previous works [17], [27], [44], [45], [46].

To thermally investigate our structure, we solved the heat diffusion equation using CST software. We set the thermal properties of the materials as in Table 3. Moreover, an open boundary condition with ambient temperature (20 °C) is used

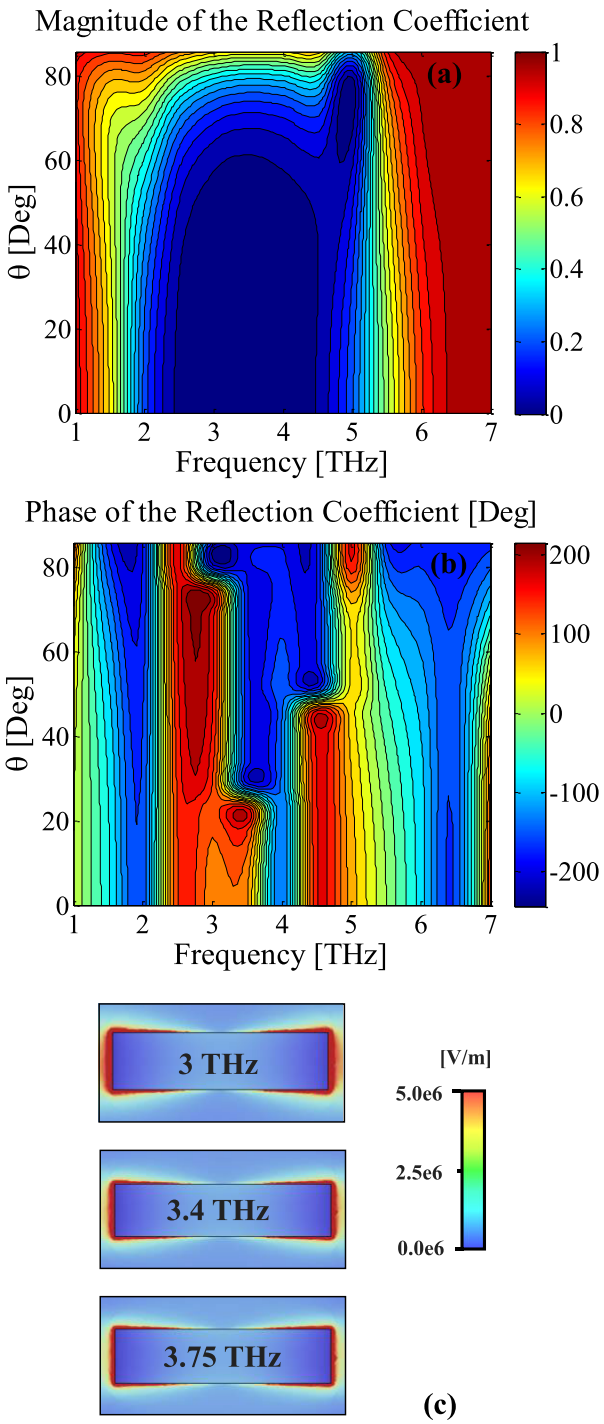

FIGURE 9. (a) The magnitude and (b) the phase of reflection of the electric field from the reconfigurable nonlocal metasurface at high temperatures as a function of frequency and angle of incidence (θ). (c) The normalized electric field of the nano-brick in the metallic state of VO_2 at frequencies of 3 THz, 3.4 THz, and 3.75 THz.

for all boundaries, while for the top and bottom boundaries, conduction and radiation heat transfer are enabled in the thermal simulation. The electric current flowing in the silver film heats the whole structure and induces a heat source at the SiO_2 layer and at the VO_2 resonator, bringing its temperature

TABLE 3. Thermal properties of the materials used in the thermal simulation of CST.

Material	Density [kg/m^3]	Thermal Conductivity [W/K/m]	Specific Heat [J/K/kg]
Ag	10490	460	233
VO_2	4570	3.6	690
SiO_2	2650	1.3	680

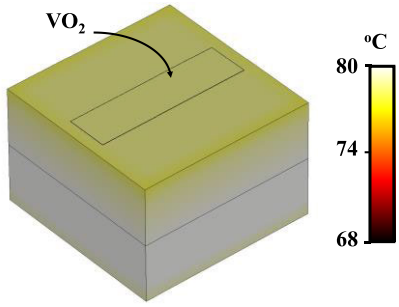

FIGURE 10. Temperature distribution in the unit cell of reconfigurable non-local metasurface with VO_2 brick resonator, SiO_2 layer, and back metal made of Ag when the heating current is flowing at the interface with silver (the ground metal layer of the structure).

to 68-80 °C (>Tc). The thermal simulation results are shown in Fig. 10, where the spatial distribution of temperature is reported in the steady state: the VO_2 resonator has a temperature larger than Tc, leading to the transition from the insulator to the metal. In other words, the heat from the electric current passes through the back metal and transfers successfully to the VO_2 resonators despite a low thermal conductivity SiO_2 layer, which is between them.

IV. CONCLUSION

In this paper, we presented an architecture of reconfigurable analog computing metasurfaces based on VO_2 brick resonators in the terahertz regime. We proposed two types of analog computing devices, one working in the k-space and the other in the real-space. The first device implements the first-order derivative at high temperatures when VO_2 resonators are in the metallic state; at low temperatures when VO_2 resonators are in the insulator state, the metasurface works like a mirror and reflects the incident wave. The second metasurface implements a second-order derivative at high temperatures and a mirror at low temperatures. In the latter case, the transformation is achieved without needing a bulk lens to convert the incident wave into k-space. Therefore, this second solution is characterized by better compactness. Moreover, this second solution shows broadband capabilities and high numerical aperture. In conclusion, the proposed metasurface paves the way toward realizing broadband and compact terahertz devices with tunable functionalities. These features make such reconfigurable metasurfaces based on VO_2 resonators appealing solutions for broadband analog computing.

REFERENCES

[1] B. Xu, G. Huang, H. Chen, X. Feng, J. Qiu, K. Luo, L. Peng, D. Liu, and P. Han, "High-NA polarization-independent isotropic spatial differential metasurface," *Photon. Nanostruct.-Fundam. Appl.*, vol. 53, Feb. 2023, Art. no. 101107.

[2] H. Rajabalipanah, A. Momeni, M. Rahmanzadeh, A. Abdolali, and R. Fleury, "Parallel wave-based analog computing using metagratings," *Nanophotonics*, vol. 11, no. 8, pp. 1561–1571, May 2022.

[3] Y. Zhou, W. Wu, R. Chen, W. Chen, R. Chen, and Y. Ma, "Analog optical spatial differentiators based on dielectric metasurfaces," *Adv. Opt. Mater.*, vol. 8, no. 4, Feb. 2020, Art. no. 1901523.

[4] C. Chen, W. Qi, Y. Yu, and X. Zhang, "On-chip optical spatial-domain integrator based on Fourier optics and metasurface," *Nanophotonics*, vol. 10, no. 9, pp. 2481–2486, Jul. 2021.

[5] D. Xu, S. Wen, and H. Luo, "Metasurface-based optical analog computing: From fundamentals to applications," *Adv. Devices Instrum.*, vol. 2022, p. 2, Jan. 2022.

[6] S. Abdollahramezani, O. Hemmatyar, and A. Adibi, "Meta-optics for spatial optical analog computing," *Nanophotonics*, vol. 9, no. 13, pp. 4075–4095, Sep. 2020.

[7] J. Wu, X. Lin, Y. Guo, J. Liu, L. Fang, S. Jiao, and Q. Dai, "Analog optical computing for artificial intelligence," *Engineering*, vol. 10, pp. 133–145, Mar. 2022.

[8] M. A. Shameli, A. D. Capobianco, L. Schenato, M. Santagiustina, and D. De Ceglia, "Wavefront control of millimeter waves with a VO_2-based reconfigurable meta-reflectarray," *IEEE Access*, vol. 11, pp. 56509–56515, 2023.

[9] M. A. Shameli, M. Magarotto, A.-D. Capobianco, L. Schenato, M. Santagiustina, and D. De Ceglia, "A reflective metalens with tunable focal length for millimeter waves," *IEEE Access*, vol. 11, pp. 104191–104199, 2023.

[10] M. A. Shameli and L. Yousefi, "Polarization-independent dielectric metasurface lens for absorption enhancement in thin solar cells," in *Proc. Bragg Gratings, Photosensitivity Poling Glass Waveguides Mater.*, 2018, Paper JTu5A.9, doi: 10.1364/BGPPM.2018.JTu5A.9.

[11] N. Yu, P. Genevet, M. A. Kats, F. Aieta, J.-P. Tetienne, F. Capasso, and Z. Gaburro, "Light propagation with phase discontinuities: Generalized laws of reflection and refraction," *Science*, vol. 334, no. 6054, pp. 333–337, Oct. 2011.

[12] A. Pors, M. G. Nielsen, and S. I. Bozhevolnyi, "Analog computing using reflective plasmonic metasurfaces," *Nano Lett.*, vol. 15, no. 1, pp. 791–797, Jan. 2015.

[13] A. Chizari, S. Abdollahramezani, M. V. Jamali, and J. A. Salehi, "Analog optical computing based on a dielectric meta-reflect array," *Opt. Lett.*, vol. 41, no. 15, p. 3451, 2016.

[14] A. Cordaro, H. Kwon, D. Sounas, A. F. Koenderink, A. Alù, and A. Polman, "High-index dielectric metasurfaces performing mathematical operations," *Nano Lett.*, vol. 19, no. 12, pp. 8418–8423, Dec. 2019.

[15] H. Kwon, D. Sounas, A. Cordaro, A. Polman, and A. Alù, "Nonlocal metasurfaces for optical signal processing," *Phys. Rev. Lett.*, vol. 121, no. 17, Oct. 2018, Art. no. 173004.

[16] N. Mohammadi Estakhri, B. Edwards, and N. Engheta, "Inverse-designed metastructures that solve equations," *Science*, vol. 363, no. 6433, pp. 1333–1338, Mar. 2019.

[17] A. Momeni, K. Rouhi, and R. Fleury, "Switchable and simultaneous spatiotemporal analog computing," 2021, *arXiv:2104.10801*.

[18] B.-X. Wang, G. Duan, W. Lv, Y. Tao, H. Xiong, D.-Q. Zhang, G. Yang, and F.-Z. Shu, "Design and experimental realization of triple-band electromagnetically induced transparency terahertz metamaterials employing two big-bright modes for sensing applications," *Nanoscale*, vol. 15, no. 45, pp. 18435–18446, 2023.

[19] Q. Yang, H. Xiong, J. H. Deng, B. X. Wang, W. X. Peng, and H. Q. Zhang, "Polarization-insensitive composite gradient-index metasurface array for microwave power reception," *Appl. Phys. Lett.*, vol. 122, no. 25, 2023, Art. no. 253901, doi: 10.1063/5.0155547.

[20] B. Wang, X. Qin, G. Duan, G. Yang, W. Huang, and Z. Huang, "Dielectric-based metamaterials for near-perfect light absorption," *Adv. Funct. Mater.*, vol. 34, no. 37, Sep. 2024, Art. no. 2402068.

[21] X. Liu, J. Zhang, B. Leng, Y. Zhou, J. Cheng, T. Yamaguchi, T. Tanaka, and M. K. Chen, "Edge enhanced depth perception with binocular meta-lens," *Opto-Electron. Sci.*, vol. 3, p. 230033-1, 2024, doi: 10.29026/oes.2024.230033.

[22] X. Zhang, Q. Chen, D. Tang, K. Liu, H. Zhang, L. Shi, M. He, Y. Guo, and S. Xiao, "Broadband high-efficiency dielectric metalenses based on quasi-continuous nanostrips," *Opto-Electron. Adv.*, vol. 7, no. 5, 2024, Art. no. 230126.

[23] X. Zhang, Y. Zhou, H. Zheng, A. E. Linares, F. C. Ugwu, D. Li, H.-B. Sun, B. Bai, and J. G. Valentine, "Reconfigurable metasurface for image processing," *Nano Lett.*, vol. 21, no. 20, pp. 8715–8722, Oct. 2021.

[24] W. Liu, M. Li, R. S. Guzzon, E. J. Norberg, J. S. Parker, M. Lu, L. A. Coldren, and J. Yao, "A fully reconfigurable photonic integrated signal processor," *Nature Photon.*, vol. 10, no. 3, pp. 190–195, Mar. 2016.

[25] H. Babashah, Z. Kavehvash, A. Khavasi, and S. Koohi, "Temporal analog optical computing using an on-chip fully reconfigurable photonic signal processor," *Opt. Laser Technol.*, vol. 111, pp. 66–74, Apr. 2019.

[26] Y. Li, W. Song, Z. Wang, H. Jiang, P. Yan, P. Lin, C. Li, M. Rao, M. Barnell, Q. Wu, and S. Ganguli, "Memristive field-programmable analog arrays for analog computing," *Adv. Mater.*, vol. 35, no. 37, 2023, Art. no. 2206648.

[27] Y. Yao, Y. Wei, J. Dong, M. Li, and X. Zhang, "Large-scale reconfigurable integrated circuits for wideband analog photonic computing," *Photonics*, vol. 10, no. 3, p. 300, Mar. 2023.

[28] J. Lourembam, A. Srivastava, C. La-o-vorakiat, H. Rotella, T. Venkatesan, and E. E. M. Chia, "New insights into the diverse electronic phases of a novel vanadium dioxide polymorph: A terahertz spectroscopy study," *Sci. Rep.*, vol. 5, no. 1, p. 9182, Mar. 2015.

[29] U. K. Chettiar and N. Engheta, "Modeling vanadium dioxide phase transition due to continuous-wave optical signals," *Opt. Exp.*, vol. 23, no. 1, p. 445, 2015.

[30] W. Kou, W. Shi, Y. Zhang, Z. Yang, T. Chen, J. Gu, X. Zhang, Q. Shi, S. Liang, F. Lan, H. Zeng, and Z. Yang, "Terahertz switchable focusing planar lens with a nanoscale vanadium dioxide integrated metasurface," *IEEE Trans. THz Sci. Technol.*, vol. 12, no. 1, pp. 13–22, Jan. 2022.

[31] J. Leroy, A. Crunteanu, A. Bessaudou, F. Cosset, C. Champeaux, and J. C. Orlianges, "High-speed metal-insulator transition in vanadium dioxide films induced by an electrical pulsed voltage over nano-gap electrodes," *Appl. Phys. Lett.*, vol. 100, no. 21, 2012, Art. no. 213507, doi: 10.1063/1.4721520.

[32] J. Qi, D. Zhang, Q. He, L. Zeng, Y. Liu, Z. Wang, A. Zhong, X. Cai, F. Ye, and P. Fan, "Independent regulation of electrical properties of VO_2 for low threshold voltage electro-optic switch applications," *Sens. Actuators A, Phys.*, vol. 335, Mar. 2022, Art. no. 113394.

[33] T. Nagatsuma, G. Ducournau, and C. C. Renaud, "Advances in terahertz communications accelerated by photonics," *Nature Photon.*, vol. 10, no. 6, pp. 371–379, Jun. 2016.

[34] Y. Zhou, X. Chen, C. Ko, Z. Yang, C. Mouli, and S. Ramanathan, "Voltage-triggered ultrafast phase transition in vanadium dioxide switches," *IEEE Electron Device Lett.*, vol. 34, no. 2, pp. 220–222, Feb. 2013.

[35] B. Scherger, C. Jördens, and M. Koch, "Variable-focus terahertz lens," *Opt. Exp.*, vol. 19, no. 5, p. 4528, 2011.

[36] J. He, J. Ye, X. Wang, Q. Kan, and Y. Zhang, "A broadband terahertz ultrathin multi-focus lens," *Sci. Rep.*, vol. 6, no. 1, p. 28800, Jun. 2016.

[37] H. S. Sehmi, W. Langbein, and E. A. Muljarov, "Optimizing the drude-lorentz model for material permittivity: Method, program, and examples for gold, silver, and copper," *Phys. Rev. B, Condens. Matter*, vol. 95, no. 11, Mar. 2017, Art. no. 115444.

[38] S. Amador-Alvarado, J. M. Flores-Camacho, A. Solís-Zamudio, R. Castro-García, J. S. Pérez-Huerta, E. Antúnez-Cerón, J. Ortega-Gallegos, J. Madrigal-Melchor, V. Agarwal, and D. Ariza-Flores, "Temperature-dependent infrared ellipsometry of Mo-doped VO_2 thin films across the insulator to metal transition," *Sci. Rep.*, vol. 10, no. 1, p. 8555, May 2020.

[39] P. B. Johnson and R. W. Christy, "Optical constants of the noble metals," *Phys. Rev. B, Condens. Matter*, vol. 6, no. 12, pp. 4370–4379, Dec. 1972.

[40] E. D. Palik, *Handbook of Optical Constants of Solids 3*. New York, NY, USA: Academic, 1998.

[41] A. Pashkin, C. Kübler, H. Ehrke, R. Lopez, A. Halabica, R. F. Haglund, R. Huber, and A. Leitenstorfer, "Ultrafast insulator-metal phase transition in VO_2 studied by multiterahertz spectroscopy," *Phys. Rev. B, Condens. Matter*, vol. 83, no. 19, May 2011, Art. no. 195120.

[42] A. Overvig and A. Alù, "Diffractive nonlocal metasurfaces," *Laser Photon. Rev.*, vol. 16, no. 8, Aug. 2022, Art. no. 2100633.

[43] Y. Zhou, S. Guo, A. C. Overvig, and A. Alù, "Multiresonant nonlocal metasurfaces," *Nano Lett.*, vol. 23, no. 14, pp. 6768–6775, Jul. 2023.

[44] D. A. Bykov, L. L. Doskolovich, E. A. Bezus, and V. A. Soifer, "Optical computation of the Laplace operator using phase-shifted Bragg grating," *Opt. Exp.*, vol. 22, no. 21, p. 25084, 2014.

[45] M. Cotrufo, A. Arora, S. Singh, and A. Alù, "Dispersion engineered metasurfaces for broadband, high-NA, high-efficiency, dual-polarization analog image processing," *Nature Commun.*, vol. 14, no. 1, p. 7078, Nov. 2023.

[46] F. Zangeneh-Nejad and A. Khavasi, "Spatial integration by a dielectric slab and its planar graphene-based counterpart," *Opt. Lett.*, vol. 42, no. 10, p. 1954, 2017.

MOHAMMAD ALI SHAMELI was born in Isfahan, Iran, in 1993. He received a B.Sc. degree in electrical engineering from Isfahan University of Technology, in 2015, and the M.Sc. and Ph.D. degrees in the fields and waves of electrical engineering from the University of Tehran, Tehran, Iran, in 2017 and 2021, respectively. He was a Postdoctoral Fellow with the Photonics and Electromagnetics Group, University of Padova, Padua, Italy, from 2022 to 2024. Currently, he is an Assistant Professor in electrical engineering-telecommunications with the K. N. Toosi University of Technology (KNTU). His research interests include electromagnetics, photonics, and metamaterials.

MIRKO MAGAROTTO (Member, IEEE) received the M.Sc. degree in aerospace engineering and the Ph.D. degree in science technology and measurements for space from the University of Padova, Padua, Italy, in 2015 and 2019, respectively. He is a Research Fellow (RTDa) with the Department of Information Engineering, University of Padova. His current research interests include plasma antennas, plasma numerical simulation, and electric space propulsion.

ANTONIO-D CAPOBIANCO (Member, IEEE) received the B.Sc. degree in electronic engineering and the Ph.D. degree in electronic and telecommunication engineering from the University of Padova, Italy, in 1989 and 1994, respectively. He is currently an Associate Professor with the Department of Information Engineering, University of Padova. His current research interests include theory and numerical modeling in the fields of photonics, plasmonics, plasma, and microwave antennas.

LUCA SCHENATO (Member, IEEE) received the M.Sc. degree in telecommunication engineering and the Ph.D. degree in electronic and telecommunication engineering from the University of Padova, Padua, Italy, in 2003 and 2007, respectively. He is currently an Assistant Professor (RTDb) with the Department of Information Engineering, University of Padova. His current research interests include optical fiber sensors, optical fiber-based devices, and more recently, metasurfaces and intelligent reflective surfaces.

MARCO SANTAGIUSTINA (Member, IEEE) received the M.Sc. degree in electronic engineering and the Ph.D. degree in electronic and telecommunication engineering from the University of Padova, Padua, Italy, in 1992 and 1996, respectively. He is currently a Full Professor with the Department of Information Engineering, University of Padova. His current research interests include nonlinear optics, optical fibers, and electromagnetic field theory.

MARIA ANTONIETTA VINCENTI (Member, IEEE) received the Laurea (summa cum laude) and Ph.D. degrees in electronic engineering from the Politecnico di Bari, Italy, in 2005 and 2009, respectively.

She is an Associate Professor with the Department of Information Engineering, University of Brescia, Italy. From 2007 to 2009, she was a Research Fellow with the U.S. Army Charles M. Bowden Laboratory, Redstone Arsenal, under several awards sponsored by the U.S. Army Forward Element Command Atlantic. From 2009 to 2012 and from 2016 to 2017, she was a Research Scientist with AEgis Technologies Inc. From 2012 to 2017, she was appointed as a Research Associate with the National Research Council, U.S. Army Aviation and Missile Research Development and Engineering Center. From 2017 to 2020, she was an Assistant Professor with the Department of Information Engineering, University of Brescia, Italy. She serves as a reviewer for international research projects funded by the U.S. Department of Defense and the Italian Ministry of Education and Research. She has authored or co-authored more than 200 peer reviewed articles and conference proceedings, three book chapters, and holds two U.S. patents. Her research interests include theoretical investigations and computational modeling of linear and nonlinear interactions in optical nanostructures, including plasmonic devices, optical sensors, low-permittivity media, 2-D materials, and sub-wavelength structures for light harvesting. She is a Senior Member of OSA and a member of SPIE and Italian Society of Electromagnetism (SiEm). She was a recipient of the "Rita Levi-Montalcini" Award for Young Researchers funded by the Italian Ministry for Education (MIUR), in 2016. She serves as a Referee for several international journals, such as *Nature Communications*, *Optics Letters*, *Optics Express*, *Journal of Optical Society of America B*, *Applied Optics*, *Journal of Optics*, *Journal of European Optical Society*, *Progress in Electromagnetics Research*, *Optics Communications*, *Journal of Applied Physics*, *ACS Photonics*, *ACS Applied Materials and Interfaces*, IEEE Photonics Journal, *Materials Research Express*, and *Scientific Reports*. She is an Associate Editor of *Optica* and *Optics Express*.

DOMENICO DE CEGLIA (Member, IEEE) received the Laurea and Ph.D. degrees in electrical engineering from the Politecnico di Bari, Italy, in 2003 and 2007, respectively. He has been a Senior Research Associate with the National Research Council of the National Academies, USA. He is currently an Associate Professor in electromagnetic fields with the University of Brescia, Italy. He has published more than 100 papers in peer-reviewed journals and proceedings of international conferences in the field of optics and photonics. His research interests include electromagnetics, optics, and photonics, with an emphasis on plasmonics and light-matter interactions in nanostructures, such as metasurface, metamaterials and nanoresonators, and nonlinear optics.

Open Access funding provided by 'Università degli Studi di Padova' within the CRUI CARE Agreement